OPTICA

Soliton molecules in femtosecond fiber lasers: universal binding mechanism and direct electronic control

Luca Nimmesgern,[1] Cornelius Beckh,[2] Hannes Kempf,[2] Alfred Leitenstorfer,[2] and Georg Herink[1,*]

[1]Experimental Physics VIII—Ultrafast Dynamics, University of Bayreuth, Bayreuth, Germany
[2]Department of Physics and Center for Applied Photonics, University of Konstanz, Konstanz, Germany
*Corresponding author: georg.herink@uni-bayreuth.de

Received 18 August 2021; revised 15 September 2021; accepted 15 September 2021 (Doc. ID 439905); published 19 October 2021

Sequences of ultrashort pulses form the basis of extremely precise laser applications ranging from femtosecond spectroscopy, to material microprocessing, to biomedical imaging. Dynamic patterns of temporal solitons—termed "soliton molecules"—inside mode-locked cavities provide yet unexplored means for generating reconfigurable arrangements of ultrashort pulses. Here, we demonstrate the external control of solitonic bound states in widespread erbium-doped fiber lasers via direct electronic modulation of the semiconductor pump source. This straightforward approach allows for switching between discrete soliton doublet states of picosecond separations, employing and relying on laser-intrinsic soliton interactions. We analyze the externally induced dynamics based on real-time switching data acquired by time-stretch dispersive Fourier transform spectroscopy and identify a universal bound-state formation mechanism different from broadly considered models. Owing to the ease of implementation and its intrinsic tunability, our control scheme is readily applicable to various laser platforms enabling, e.g., rapid multipulse measurements and tailored nonlinear light–matter interactions.

https://doi.org/10.1364/OPTICA.439905

1. INTRODUCTION

Advanced laser applications in science and technology rely on composing, modulating, and manipulating complex ultrashort pulse patterns in order to provide frequency-swept excitation, low-noise detection, and nonlinear light–matter interactions [1–3]. Intriguingly, multipulse operation and complex interactions are being reported for virtually all implementations of passive mode locking. Yet the intrinsic dynamics have been barely experimentally controlled nor practically exploited so far.

Recently, real-time spectroscopy based on time-stretch dispersive Fourier transform (TS-DFT) [4] has been introduced for resolving such multipulse dynamics in mode-locked oscillators [5,6], revealing a wealth of previously hidden, transient multisoliton dynamics including stable and meta-stable soliton binding [7–10], soliton split-up and (multicolor) collision [11,12], harmonic mode locking [13], breathing dissipative solitons [14], and multisoliton molecular complexes [15,16] to name a few recent examples. Moreover, resonances of soliton bound states and the switching between two bound states have been reported [17] based on modulation of the optical pump beam intensity in a Ti:sapphire solid-state laser.

Mode-locked erbium-doped fiber (Er:fiber) lasers present compact, adaptable, and well-established ultrafast sources [18,19] using widespread network components at telecom wavelength. A broad range of mode-locking schemes has been demonstrated, featuring implementations via saturable absorber mode locking in bulk crystals, semiconductor absorber mirrors, nonlinear polarization rotation, nonlinear amplifying loop mirrors, and more [18,19]. As a result, Er:fiber lasers are established as a key model system for intracavity pulse dynamics in mode-locked sources [20,21]. In particular, pumping with semiconductor lasers enables fast and direct electronic modulation via miniaturized and low-cost pump sources for telecom amplifiers as employed previously in carrier-envelope stabilization of optical frequency combs [22].

Here, we demonstrate rapid external control of soliton bound states in a saturable-absorber mode-locked Er:fiber laser via direct electronic modulation of the pump power as sketched in Fig. 1(a).

2. RESULTS

A. External Perturbation

In the experiment, we initiate dual-pulse operation at the laser startup and implement a laser perturbation via current modulation of the semiconductor diode-laser driver. The electronic control signal is generated with an arbitrary waveform generator (AWG) and coupled to the laser driver circuit. The output signal of the 980 nm stabilized semiconductor laser allows for modulation bandwidths exceeding 10 MHz with a fall time of the pump power below 22 ns.

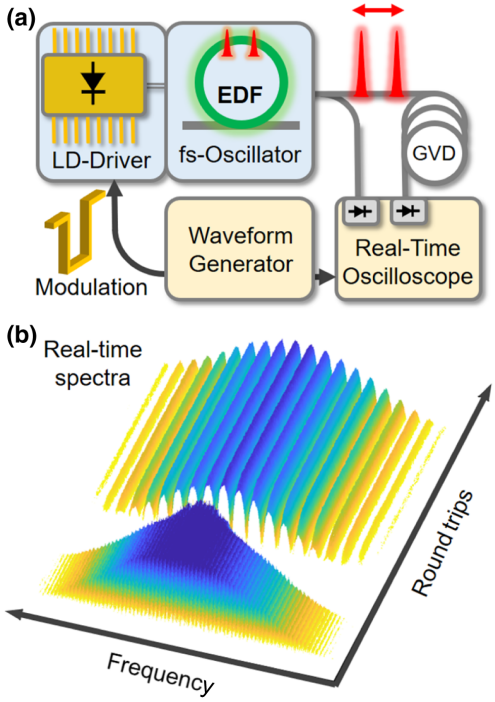

Fig. 1. (a) Experimental scheme: A mode-locked oscillator based on erbium-doped fiber (EDF) is directly controlled via electronic modulation of a semiconductor pump laser-diode (LD). Switching between multisoliton states is captured in real time via dispersive Fourier transform spectroscopy, exploiting a dispersive fiber (GVD) and real-time photodetection. (b) Round-trip-resolved real-time spectral interferograms are recorded during modulation as a function of consecutive laser round trips and reveal stable bound states, encoded via spectral interference fringes.

The fiber oscillator is implemented in a ring resonator and incorporates passive mode locking via a semiconductor saturable absorber mirror (SAM) [23,24]. The typical mode of operation generates isolated solitary pulses of ∼500 fs duration at a repetition rate of 40 MHz.

We characterized the transfer dynamics of the intracavity pulse energy via sinusoidal cw-pump modulation, yielding modulation transfer up to a bandwidth of approximately 8 kHz. The transfer function corresponds to damped gain relaxation oscillations governed by the millisecond upper-state lifetime and high saturation energy. In the temporal domain, the intracavity energy displays a fall time of 29 μs upon transient reduction of the pump power via rectangular functions of varying durations as shown in Figs. 2(a) and 2(b), compatible with the gain relaxation oscillations around 10 kHz. We achieve a rapid perturbation of single-pulse operation by applying a sufficient external pump power reduction in order to initially induce and then to switch multipulse states. We map the transition between stable single-pulse and multipulse operation as a function of perturbation strengths, given by the cumulative pump energy reduction via drop depth ΔP and drop duration τ. This transition map, displayed in Fig. 2(c), allows for the selection of control parameter values. As apparent in this representation, we achieve effective perturbation at a constant cumulative pump energy reduction given by the product $\Delta P \cdot \tau$ and marked by the black line. The cumulative reduction corresponds to around 3% of the laser saturation energy.

B. Switching and Real-Time Spectroscopy

Starting at a stable bound state of two solitons, we rapidly switch between two dominant bound states (I and II) via injection of the control signal, i.e., via transient reduction of pump power. We track the resultant multisoliton dynamics via real-time detection with the TS-DFT spectral interferometry and a fast photodetector. The real-time oscilloscope features analog bandwidths of 16 GHz at 100 GSa sampling rate, and the group velocity dispersion (GVD) is set to 990 ps/nm. We trigger every real-time acquisition event via the corresponding external electrical modulation waveform.

The round-trip-resolved spectral interferograms and corresponding field autocorrelations (Fourier amplitudes of the spectra) synchronous to the external control signal of single switching events are shown in Figs. 3(a) and 3(b). Switching occurs from a stable bound state at 55.3 ps (state I) to a shorter binding separation of 14.5 ps (state II) via transient dissociation of the initial bound state. We assume a common central wavelength of 1567 nm for both pulses, in agreement with the extracted separations from scanning interferometric autocorrelations (see Supplement 1). The dissociation of the bound states requires sufficient reduction of intracavity energy, allowing for the transient induction of single-pulse operation. Subsequently, following the recovery of the pump energy, the single soliton experiences excess gain apparent as rapid spectral broadening and a power overshoot in the time-resolved spectra. At this stage, a new second soliton forms via

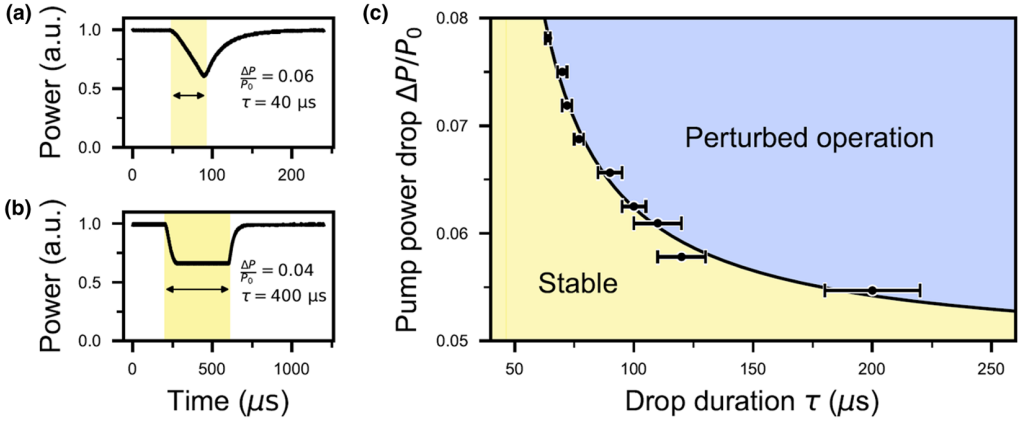

Fig. 2. (a) Temporal evolution of the oscillator power upon fast pump modulation via a 40 μs drop, evidencing the transient fall and rise times. (b) Corresponding waveform for longer pump modulation. (c) Stability map of oscillator operation upon perturbation via drops in pump power at given amplitude and duration. Efficient perturbation is achieved at a constant product of reduction amplitude and respective duration (black line).

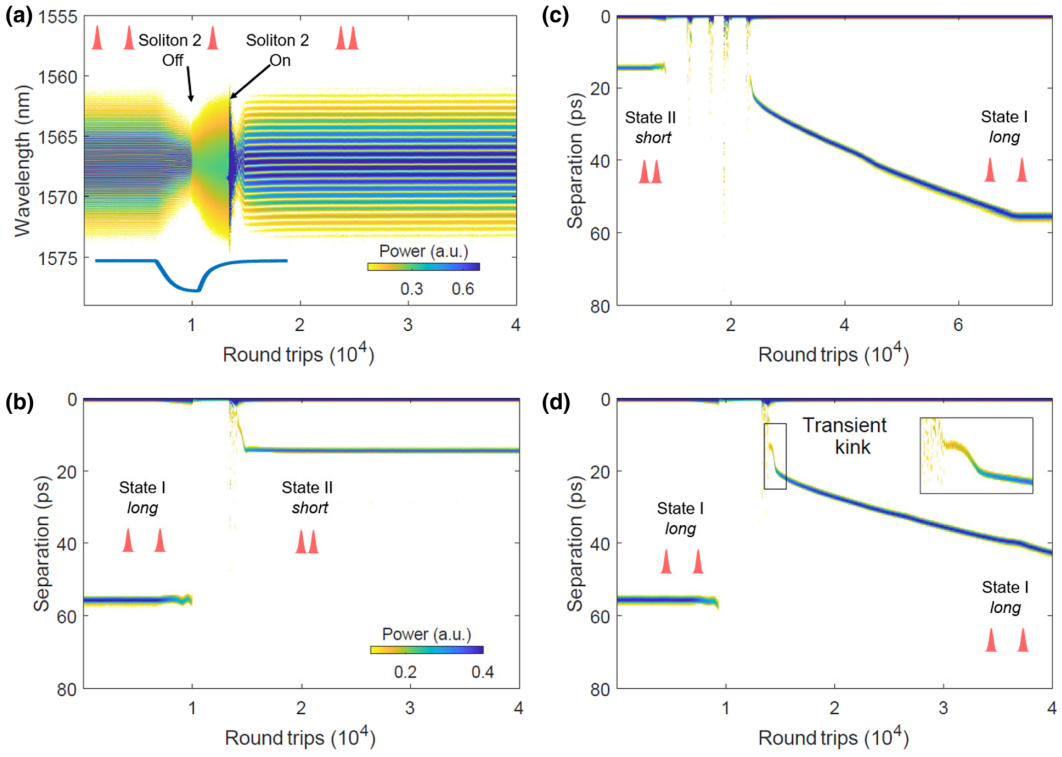

Fig. 3. (a) Real-time spectra during switching from state I (long separation) to state II (short separation). Transient reduction of intracavity energy (inset) dissolves the second soliton, apparent in a loss of fringe visibility. Upon rapid energy recovery, the second soliton is reinitiated and binds at a shorter separation. The corresponding field autocorrelations obtained via Fourier transformation of the interferograms are synchronously displayed in (b). (c) The reverse switching process from state II to the longer separation state I. (d) This event reveals the switching from state I back to the initial state, displaying the alternative event of bound state reinitiation. In addition, a transient kink indicates an instable binding separation at around 10 ps (extended view in the inset).

split-up from the first seeding pulse and, effectively, regenerates two closely spaced unbound pulses out of equilibrium. The corresponding autocorrelations in Fig. 3(b) resolve the trajectories of their intersoliton motion. The speed of relative motion is linked to the effective gain gradient experienced by the two succeeding pulses [25]. Prior to full recovery, the second soliton experiences a lower gain gradient as compared to the leading pulse, and thus the relative motion is fast. Upon full recovery, the second pulse saturates the gain comparably to the leading soliton, and the relative motion rapidly decreases. In case of no further interactions, multiple solitons typically stabilize in an equidistant harmonically mode-locked state.

As the soliton splitting and reformation of the double-pulse state arise from fluctuations, each individual event exhibits varying spectro-temporal dynamics that translate to different relative soliton motion in the early phase of the process.

Hence, soliton binding and stabilization occur either at the close separation τ_{II} or later at the longer separation τ_I, depending on the exact equilibration of the soliton intensities. This enables reverse switching between the short τ_{II} and the long separation τ_I as shown in the switching event of Fig. 3(c). Additionally, the regeneration of an initial state may be obtained as the alternative trajectory as shown in the example of Fig. 3(d). This dataset also displays a transient kink, revealing an instable binding separation at around 10 ps (extended view in the inset). Based on the employed strong perturbation via transient single-pulse operation, the reinitiation of the bound states is determined by subtle fluctuations. A tailored perturbation may enable the deterministic switching between bound states in analogy to results with Ti:sapphire solid-state lasers in a different regime [17].

We note that the relaxation to the stable separation in Fig. 3(d) was not entirely captured within this real-time dataset due to limited acquisition length, but the final state was given by the long separation of state I.

C. Universal Binding Mechanism

We now discuss the origin of soliton interactions and bound-state formation with general implications to a broad set of mode-locked laser sources. Attraction and repulsion of ultrashort temporal solitons in optical fiber may induce bound states of solitons or "soliton molecules," discovered as a result of direct interaction between closely spaced pulses [26] or upon long-range interaction, i.e., via dispersive waves [27]. Pulse evolution in mode-locked lasers—with additional gain, loss, and saturable absorption—is often described in the context of modified nonlinear Schrödinger equations or complex Ginzburg–Landau equations, and various bound states were found theoretically [28–33], yet the stability of these might vary significantly [34]. Experimentally, various resembling dynamics were observed in different systems, particularly reported within a large body of fiber laser studies (examples in Refs. [15,35–39]). Despite highly reproducible experimental observations and remarkable insensitivity to the actual state of laser operation [36], the key experimental observable—the actual bound-state separation—is commonly not explained or quantitatively predicted by theoretical models. In contrast, the bound

states mediated by reflected transverse acoustic waves in fibers present one rather exceptional mechanism in which theories are able to precisely account for experimental bound-state separations [16,40–43]. Still, the interaction is subtle, and its importance often arises in long-range propagation or in custom-designed fibers [16,42].

Here, we identify a universal mechanism of temporal soliton bound-state formation akin to additive-pulse mode locking: A fraction of the leading soliton reflects at an optical interface of the cavity and counterpropagates to an adjacent interface. Following a second reflection, an "echo" is formed, which copropagates with the leading soliton and reaches the SAM with a time delay given by the twofold optical path length between both surfaces as sketched in Fig. 4 (green). Eventually, a second, initially unbound trailing soliton temporally superposes with the echo at the saturable absorber. As a result, the second soliton experiences slightly reduced nonlinear absorption, breaking the translational symmetry and stabilizing the soliton bound state at the distinguished separation. The mechanism can be considered as "long-range" binding without direct overlap of the pulses, and bound-state separations can range from few 100 fs up to the round-trip duration of several 10 ns. The mechanism is not limited to mode-locked lasers with saturable absorbers but applies to any ultrafast amplitude modulation.

In our experiments, the observed dominant bound-state separations are $\tau_I = 55.3$ ps and $\tau_{II} = 14.5$ ps. An analysis of intracavity feedback from the employed resonator components (detailed in Supplement 1) reveals that the shorter separation matches within the experimental accuracy to the round-trip propagation delay between the free-space path length between the SAM and the adjacent focusing lens surface of 15.9 ps or $2 \cdot 2.38$ mm/c with the vacuum speed of light c. The finite reflectivity of the antireflective-coated lens surface is specified to below 0.5%. The round-trip duration and path length between the SAM and the opposing surface of the aspherical lens coincides with this separation of 54.7 ps or $(2 \cdot 2.38\ \text{mm} + 2 \cdot 1.6 \cdot 3.64\ \text{mm})/c$, with the group index of the lens material of 1.6 (see the sketch in Supplement 1). We performed sensitive linear autocorrelation measurements in single-pulse operation using an external scanning Michelson interferometer. The separations between subtle echo features match the separations obtained during bound-state operation. In addition, we detect a subtle delayed echo at around 10 ps that coincides with the characteristic transient kink or position of preferred restart of the second pulse in the real-time trajectories [see Figs. 3(b) and 3(d)]. This feature matches to backreflections inside the fiber-optical circulator between the collimator and the polarizer of ∼1.5 mm separation (see Supplement 1).

Whereas mode-locking dynamics in regular single-pulse operation are typically not impaired by spurious impedance mismatch due to the nonlinear "winner-takes-all" dynamics, here, the impact of such reflections onto multipulse interactions is of essential importance: a second soliton sensitively probes cavity perturbations from delayed temporal responses of intracavity components upon its relative motion. The adequate consideration of surface reflections appears yet to be largely missing in various discussions on soliton bound-state generation in a broad set of publications investigating soliton interactions in mode-locked lasers. Widely employed polarization optics and nonreciprocal elements, including fiber-optic isolators or circulators, typically include eight or more interfaces between different materials of millimeter (mm) lengths. Moreover, we note that our observations indicate no significant contributions from higher-order dispersion or nonlinear effects, dispersive wave interactions, nor acoustic feedback as primary sources of soliton binding. Consequently, previous lumped models that do not include the actual multicomponent laser structure are not capable of analyzing and predicting the bound-state separations frequently encountered in actual laser sources.

We emphasize that our proposed soliton coupling mechanism is based on linear reflections and thus features increased stability compared to potential interactions arising from higher-order effects [36]—whereas the latter sensitively depend on specific laser operation parameters, i.e., on pump power, dispersion, and peak intensities. Hence, our observations represent universal dynamics that are relevant for various mode-locked sources featuring multipulse interaction due to intracavity feedback.

D. Tunable Bound States

Finally, we directly apply the presented mechanism for the generation of variably tunable bound states. We insert an antireflective-coated thin plate (90 μm thickness, 0.1% reflectivity at 1550 nm) in the free-space section of the resonator prior to the focusing lens of the SAM. Using a mechanical delay stage, we are able to shift the plate along the propagation direction, effectively increasing the distance to the SAM. Upon initial perturbation or restart, we observe the formation of a novel bound state, the temporal separation of which is tunable via mechanically shifting the plate as presented in Fig. 4(b). We extracted the tunable separations from spectral interferograms as shown in Supplement 1. The slope is given by the free-space propagation

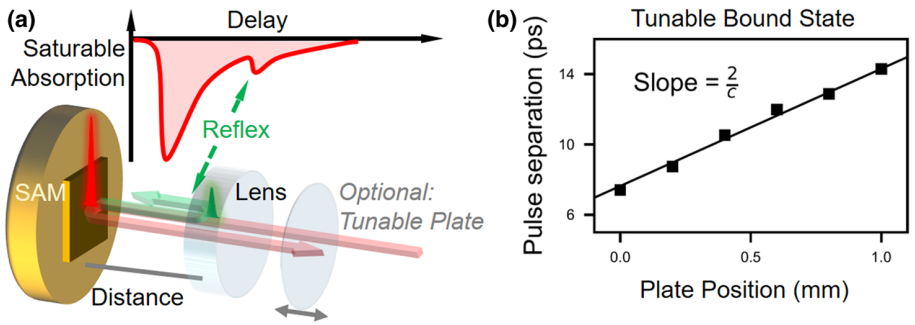

Fig. 4. (a) Illustration of the binding mechanism: Copropagating reflexes from intracavity surfaces introduce subtle delayed depletions in the saturable absorption, sketched in the transient response (top). At temporal overlap with these reflections, a subsequent trailing soliton experiences reduced loss and stabilizes at the corresponding delay. An optional thin plate is introduced for generation of a tunable separation to the SAM. (b) Upon insertion of the optional plate, the separation of the new stable bound state is tuned via translation of the plate position.

delay for a roundtrip as $2/c$. At this stage, we observe that the laser operation may be disturbed upon coarse mechanical intracavity motion, and the solitons may internally regroup or switch within the set of dominant bound-state separations.

3. CONCLUSIONS

In conclusion, we have experimentally demonstrated the rapid control of ultrashort soliton bound states via direct electronic modulation of the semiconductor pump-laser power, enabling the switching between two stable soliton-doublet states. Employing real-time spectroscopy, we map the switching trajectories and identify finite reflective feedback from intracavity components as the origin of bound-state separations, generating stable and highly reproducible temporal soliton separations. Moreover, we demonstrate the tunable generation of stable bound states via translation of an additional reflective intracavity plate. Given the ease of implementation and the flexible tunability of ultrashort separations, this versatile scheme appears highly applicable for future multipulse laser applications in high-speed measurements and nonlinear light–matter interactions.

Funding. Deutsche Forschungsgemeinschaft (project number 461131168); University of Bayreuth funding programme for Open Access Publishing.

Acknowledgment. We gratefully thank Sarah Hutter, Stefan Eggert, and Robert Weiner for technical support, and Dieter Brüggemann and Markus Lippitz for providing measurement equipment.

Disclosures. The authors declare no conflicts of interest.

Data Availability. Data underlying the results presented in this paper are available from the authors upon reasonable request.

Supplemental document. See Supplement 1 for supporting content.

REFERENCES

1. A. H. Zewail, "Femtochemistry: atomic-scale dynamics of the chemical bond," J. Phys. Chem. A **104**, 5660–5694 (2000).
2. M. Malinauskas, A. Žukauskas, S. Hasegawa, Y. Hayasaki, V. Mizeikis, R. Buividas, and S. Juodkazis, "Ultrafast laser processing of materials: from science to industry," Light Sci. Appl. **5**, e16133 (2016).
3. C. H. Camp, Jr. and M. T. Cicerone, "Chemically sensitive bioimaging with coherent Raman scattering," Nat. Photonics **9**, 295–305 (2015).
4. A. Mahjoubfar, D. V. Churkin, S. Barland, N. Broderick, S. K. Turitsyn, and B. Jalali, "Time stretch and its applications," Nat. Photonics **11**, 341–351 (2017).
5. G. Herink, F. Kurtz, B. Jalali, D. R. Solli, and C. Ropers, "Real-time spectral interferometry probes the internal dynamics of femtosecond soliton molecules," Science **356**, 50–54 (2017).
6. K. Krupa, K. Nithyanandan, U. Andral, P. Tchofo-Dinda, and P. Grelu, "Real-time observation of internal motion within ultrafast dissipative optical soliton molecules," Phys. Rev. Lett. **118**, 243901 (2017).
7. S. Hamdi, A. Coillet, and P. Grelu, "Real-time characterization of optical soliton molecule dynamics in an ultrafast thulium fiber laser," Opt. Lett. **43**, 4965–4968 (2018).
8. Y. Zhou, Y.-X. Ren, J. Shi, and K. K. Y. Wong, "Breathing dissipative soliton explosions in a bidirectional ultrafast fiber laser," Photon. Res. **8**, 1566–1572 (2020).
9. J. Zeng and M. Y. Sander, "Real-time transition dynamics between multipulsing states in a mode-locked fiber laser," Opt. Lett. **45**, 5–8 (2020).
10. M. Suzuki, O. Boyraz, H. Asghari, and B. Jalali, "Spectral dynamics on saturable absorber in mode-locking with time stretch spectroscopy," Sci. Rep. **10**, 14460 (2020).
11. P. Ryczkowski, M. Närhi, C. Billet, J.-M. Merolla, G. Genty, and J. M. Dudley, "Real-time full-field characterization of transient dissipative soliton dynamics in a mode-locked laser," Nat. Photonics **12**, 221–227 (2018).
12. Y. Wei, B. Li, X. Wei, Y. Yu, and K. K. Y. Wong, "Ultrafast spectral dynamics of dual-color-soliton intracavity collision in a mode-locked fiber laser," Appl. Phys. Lett. **112**, 081104 (2018).
13. X. Liu and M. Pang, "Revealing the buildup dynamics of harmonic mode-locking states in ultrafast lasers," Laser Photon. Rev. **13**, 1800333 (2019).
14. J. Peng, S. Boscolo, Z. Zhao, and H. Zeng, "Breathing dissipative solitons in mode-locked fiber lasers," Sci. Adv. **5**, eaax1110 (2019).
15. Z. Q. Wang, K. Nithyanandan, A. Coillet, P. Tchofo-Dinda, and P. Grelu, "Optical soliton molecular complexes in a passively mode-locked fibre laser," Nat. Commun. **10**, 830 (2019).
16. W. He, M. Pang, D. H. Yeh, J. Huang, C. R. Menyuk, and P. St. J. Russell, "Formation of optical supramolecular structures in a fibre laser by tailoring long-range soliton interactions," Nat. Commun. **10**, 5756 (2019).
17. F. Kurtz, C. Ropers, and G. Herink, "Resonant excitation and all-optical switching of femtosecond soliton molecules," Nat. Photonics **14**, 9–13 (2020).
18. M. E. Fermann, A. Galvanauskas, G. Sucha, and D. Harter, "Fiber-lasers for ultrafast optics," Appl. Phys. B **65**, 259–275 (1997).
19. D. Brida, G. Krauss, A. Sell, and A. Leitenstorfer, "Ultrabroadband Er:fiber lasers," Laser Photon. Rev. **8**, 409–428 (2014).
20. A. B. Grudinin, D. J. Richardson, and D. N. Payne, "Energy quantisation in figure eight fibre laser," Electron. Lett. **28**, 67–68 (1992).
21. B. G. Bale, K. Kieu, J. N. Kutz, and F. Wise, "Transition dynamics for multi-pulsing in mode-locked lasers," Opt. Express **17**, 23137–23146 (2009).
22. N. Haverkamp, H. Hundertmark, C. Fallnich, and H. R. Telle, "Frequency stabilization of mode-locked Erbium fiber lasers using pump power control," Appl. Phys. B **78**, 321–324 (2004).
23. U. Keller, J. Weingarten, F. X. Kartner, D. Kopf, B. Braun, D. Jung, R. Fluck, C. Honninger, N. Matuschek, and J. Aus der Au, "Semiconductor saturable absorber mirrors (SESAM's) for femtosecond to nanosecond pulse generation in solid-state lasers," IEEE J. Sel. Top. Quantum Electron. **2**, 435–453 (1996).
24. U. Keller, "Recent developments in compact ultrafast lasers," Nature **424**, 831–838 (2003).
25. H. M. Bensch, G. Herink, F. Kurtz, and U. Morgner, "Harmonically mode-locked Yb:CALGO laser oscillator," Opt. Express **25**, 14164–14172 (2017).
26. F. M. Mitschke and L. F. Mollenauer, "Experimental observation of interaction forces between solitons in optical fibers," Opt. Lett. **12**, 355–357 (1987).
27. K. Smith and L. F. Mollenauer, "Experimental observation of soliton interaction over long fiber paths: discovery of a long-range interaction," Opt. Lett. **14**, 1284–1286 (1989).
28. B. A. Malomed, "Bound solitons in coupled nonlinear Schrödinger equations," Phys. Rev. A **45**, R8321–R8323 (1992).
29. W. Schöpf and L. Kramer, "Small-amplitude periodic and chaotic solutions of the complex Ginzburg-Landau equation for a subcritical bifurcation," Phys. Rev. Lett. **66**, 2316–2319 (1991).
30. N. Akhmediev, A. Ankiewicz, and J. Soto-Crespo, "Multisoliton solutions of the complex Ginzburg-Landau equation," Phys. Rev. Lett. **79**, 4047–4051 (1997).
31. A. Komarov and F. Sanchez, "Structural dissipative solitons in passive mode-locked fiber lasers," Phys. Rev. E **77**, 066201 (2008).
32. A. Zavyalov, R. Iliew, O. Egorov, and F. Lederer, "Dissipative soliton molecules with independently evolving or flipping phases in mode-locked fiber lasers," Phys. Rev. A **80**, 043829 (2009).
33. G. Kozyreff and L. Gelens, "Cavity solitons and localized patterns in a finite-size optical cavity," Phys. Rev. A **84**, 023819 (2011).
34. V. V. Afanasjev and N. Akhmediev, "Soliton interaction in nonequilibrium dynamical systems," Phys. Rev. E **53**, 6471–6475 (1996).
35. P. Grelu, F. Belhache, F. Gutty, and J.-M. Soto-Crespo, "Phase-locked soliton pairs in a stretched-pulse fiber laser," Opt. Lett. **27**, 966–968 (2002).
36. D. Tang, B. Zhao, L. Zhao, and H. Tam, "Soliton interaction in a fiber ring laser," Phys. Rev. E **72**, 016616 (2005).
37. M. Grapinet and P. Grelu, "Vibrating soliton pairs in a mode-locked laser cavity," Opt. Lett. **31**, 2115–2117 (2006).
38. L. M. Zhao, D. Y. Tang, X. Wu, D. J. Lei, and S. C. Wen, "Bound states of gain-guided solitons in a passively mode-locked fiber laser," Opt. Lett. **32**, 3191–3193 (2007).
39. B. Ortaç, A. Zaviyalov, C. K. Nielsen, O. Egorov, R. Iliew, J. Limpert, F. Lederer, and A. Tünnermann, "Observation of soliton molecules with

independently evolving phase in a mode-locked fiber laser," Opt. Lett. **35**, 1578–1580 (2010).
40. E. M. Dianov, A. V. Luchnikov, A. N. Pilipetskii, and A. M. Prokhorov, "Long-range interaction of picosecond solitons through excitation of acoustic waves in optical fibers," Appl. Phys. B **54**, 175–180 (1992).
41. A. N. Pilipetskii, E. A. Golovchenko, and C. R. Menyuk, "Acoustic effect in passively mode-locked fiber ring lasers," Opt. Lett. **20**, 907–909 (1995).
42. J. K. Jang, M. Erkintalo, S. G. Murdoch, and S. Coen, "Ultraweak long-range interactions of solitons observed over astronomical distances," Nat. Photonics **7**, 657–663 (2013).
43. M. Erkintalo, K. Luo, J. K. Jang, S. Coen, and S. G. Murdoch, "Bunching of temporal cavity solitons via forward Brillouin scattering," New J. Phys. **17**, 115009 (2015).